Di Felice *et al. Biology Direct* (2025) 20:63
https://doi.org/10.1186/s13062-025-00656-5

Biology Direct

RESEARCH Open Access

Allosteric modulation of Grb2 drives ligand-dependent signal responses

Mariana Di Felice[1,2], Lucrezia Romana Rolfi[1,2], Julian Toso[1,2], Valeria Pennacchietti[1,2], Eduarda S. Ventura[1,2], Angelo Toto[1,2], Antonella Tramutola[1,2] and Stefano Gianni[1,2*]

Abstract
Adaptor proteins play a crucial role in signal transduction by facilitating the assembly of protein complexes at specific subcellular domains. These multifunctional molecules contain multiple binding modules that enhance the efficiency and flexibility of cellular signaling pathways, thereby orchestrating complex responses. Among these proteins, Grb2 (growth factor receptor–bound protein 2) emerges as a key regulator owing to its unique "sandwich" structure. Despite lacking intrinsic enzymatic activity, recent investigations have revealed that Grb2 acts not merely as a passive bridge but also utilizes intramolecular allosteric communication to modulate binding specificity. In this study, we compared the kinetic binding properties of SH2-SH3 belonging to Grb2 with Gab2 and the same experiment with bound states of the SH2 domain using two different peptides that mimics the physiological ligands of SH2. Our results demonstrate that the SH2 domain plays a critical regulatory role, exhibiting remarkably distinct behaviors in free and bound states, and depending on the ligand it binds to. This suggests how selectivity can be modulated by intradomain allostery. In vitro functional assays measuring the activation levels of the target protein further supported our hypothesis.

Keywords Adaptor proteins, Kinetics, Allostery, Site-directed mutagenesis

Introduction

Many molecular pathways are mediated by adaptor proteins. This class of macromolecules typically lacks intrinsic enzymatic or catalytic activity and facilitates the recruitment of protein-binding partners to specific subcellular domains. Adaptor proteins are essential cellular components that govern intricate signaling pathways in time and space with precise specificity and facilitate the transmission of information from extracellular signals to intracellular effectors [1–4]. They exert their functions thanks to their modular nature, typically comprising multiple protein-binding modules [5–7]. These features confer the ability to bring multiple signaling molecules into proximity, thereby ensuring the efficiency and flexibility of signaling and allow orchestrating complex signal transduction pathways.

Grb2, also known as growth factor receptor–bound protein 2, is a central player among adapter proteins, playing a pivotal role in regulating signaling cascades from cell surface receptors to cellular responses in several oncogenic signaling pathways [8–12]. Grb2 is at the core of a complex network of signals, it plays a key role in regulating essential cellular processes like growth, differentiation, and survival [13–16]. This crucial adaptor protein is well-known for its ability to connect the epidermal growth factor receptor tyrosine kinase (RTK) to

*Correspondence:
Stefano Gianni
stefano.gianni@uniroma1.it
[1]Dipartimento di Scienze Biochimiche "A. Rossi Fanelli", Sapienza Università di Roma, P.le Aldo Moro 5, Rome 00185, Italy
[2]Laboratory affiliated to Istituto Pasteur Italia - Fondazione Cenci Bolognetti, Rome, Italy

the activation of RAS and its downstream kinases such as that of the protein kinese B, also known as Akt [8–10, 17].

The human Grb2 protein, with a molecular weight of 25 kDa, comprises 217 amino acids and exhibits a distinctive "sandwich structure" [18]. This dynamic structure includes a central SH2 domain composed of 93 amino acids from 60 to 152 can interact directly with receptor tyrosine kinases and non-receptor tyrosine kinases such as ligand with phospho-tyrosine consensus motif pYxNx flanked by two Src homologous 3 (SH3) domains on each side. The SH3 domains in Grb2, comprising the carboxyl-terminal SH3 (C-SH3) domain (residues 1–58) and the amino-terminal SH3 (N-SH3) domain (residues 156–215), are both capable of recognizing proline-rich sequences, such as PxxP motifs, and function as a linker between the SH2 domain and downstream proteins.

Adaptor proteins are often shallowly considered as passive adaptors mediating intermolecular binding. But, more detailed analyses of their functions have revealed that complex communication pathways may occur between their consistent domains, thereby invoking the concept of 'allosteric communication pathways' [19–21]. The classic concept of allostery suggests that a detectable conformational change regulates the affinity for a specific ligand [22, 23], but allosteric communication can even occur without any obvious change in conformation [24] and, therefore, allostery should be addressed primarily from an energetic rather than a structural perspective [25–27]. In the case of Grb2 we have recently demonstrated that an allosteric network, at interface between C-SH3 domain and the SH2 domain, regulates the binding selectivity of C-SH3 domain [28]. These findings reinforce the idea that allostery serves as a key regulatory mechanism in Grb2, particularly involving the SH2 and C-SH3 domains [14, 29, 30]. In this context, it is noteworthy that while the sequence identity of these two domains is highly conserved across mammals, the N-SH3 domain appears to be structurally dispensable and is sometimes truncated or absent in certain species [14], suggesting a degree of evolutionary flexibility in the modular organization of Grb2.

To scrutinize in detail the allosteric communication pathways, we investigated here the interaction between the C-SH3 domain and its adjacent SH2 domain in Grb2, along with a peptide mimicking a segment of Gab2 (Grb2-associated binding protein 2), a scaffolding protein implicated in cellular signaling and cancer progression [31–33]. To gain deeper insight into the role of the SH2 domain, we compared previous experimental data on the SH2-SH3 interaction with Gab2 [28] and conducted analogous experiments in which the SH2 domain was in a bound state, using two phospho-tyrosine peptides that mimic its physiological ligands. Our findings reveal that the selectivity of the C-SH3 domain is not only influenced by the presence of the SH2 domain but also by whether SH2 is in its free or bound state. Moreover, we found that the specific ligand bound to SH2 dictates distinct responses in SH3, highlighting a nuanced communication pathway between these domains. To further investigate the biological relevance of these findings, we carried out experiments on HEK293 cell line and discovered that the two phospho-peptides induce different effects on the Akt activation. This result is particularly surprising given the high structural similarity of the peptides, suggesting that even subtle variations in SH2 binding can lead to distinct downstream signaling outcomes. These findings provide new insights into the intricate regulatory mechanisms governing SH2-SH3 interactions and their impact on critical signaling pathways.

Results and discussion

An intriguing question emerging from the study of adaptor proteins is whether their modular structure influences the molecular mechanisms governing the binding of their constituent domains. The case of Grb2 is particularly insightful, as (i) this protein serves as a crucial target for various types of human cancers and (ii) the comparison between the functional behavior of its isolated domains with more complex constructs revealed the presence of detectable energetic communication between its central SH2 domain and the C-terminal SH3 domain [28]. To further investigate this phenomenon, we resorted to examine the binding properties of the tandem SH2-SH3 with Gab2 and conducted the same experiments under conditions where the SH2 domain was pre-bound to two distinct ligands, namely two peptides mimicking alternatively the physiological partners Shp-2 and Irs-1. This approach offers the possibility to explore whether ligand binding to SH2 introduces an additional layer of fine regulation affecting the interaction with the C-terminal SH3 domain.

Different SH2 ligands exert a specific effect on the contiguous SH3 domain

We conducted kinetic binding experiments using a stopped-flow apparatus. This involved rapidly mixing a fixed concentration of SH2–SH3 (2 μM) with increasing concentrations (ranging from 2 to 14 μM) of a peptide mimicking Gab2, corresponding to residues 503 to 524 ($Gab2_{503-524}$). The experiments were alternatively carried out the presence of two peptides mimicking physiological partners Shp-2 and Irs-1 corresponding to residues 529–551 and 885–906, respectively. The binding kinetics traces were followed spectroscopically by measuring the change in fluorescence upon binding of Trp 194 and Trp 195 residues of C-SH3 Grb2, as reported previously [34]. All kinetic traces were fitted to a single-exponential

equation to determine the observed rate constants k_{obs}, which were then plotted as a function of $Gab2_{503-524}$ concentration. The data were analyzed using a linear equation, where the slope and y-intercept correspond to the microscopic association k_{on} and dissociation k_{off} rate constants, respectively. The binding affinity was calculated as $K_D = k_{off} / k_{on}$.

A superposition between the observed kinetics of binding to Gab2 of SH2–SH3 in the absence and in the presence of Shp-2 and Irs-1 is reported in Fig. 1. Notably, while the presence of Irs-1 does not significantly alter the binding kinetics, the inclusion of Shp-2 leads to subtle yet detectable changes in the kinetic parameters. Specifically, the overall dissociation constant K_D increases from 2.3 ± 0.5 μM to 4.3 ± 0.8 μM. This finding suggests that ligand binding to the SH2 domain can influence the interaction of the SH3 with Gab2 in a manner that is not merely passive, but rather dependent on the identity of the ligand.

Mapping the communication between domains via double mutant cycles

The results depicted in Fig. 1 are particularly intriguing as they imply that SH2 binding exerts a regulatory effect on SH3, and that this modulation is not uniform across different ligands. Instead, it appears that distinct ligands can differentially influence the functional coupling between SH2 and SH3, pointing to a mechanism of fine regulation beyond a simple allosteric interaction. Understanding the molecular underpinnings of these effects demands further investigation, particularly to dissect the nature of the energetic coupling between the domains.

A powerful approach to probe these interactions lies in the so-called 'double-mutant cycle analysis' [26, 35, 36], which allows for a quantitative assessment of how perturbations in the SH2 domain impact SH3 binding affinity and kinetics. In principle, a double mutant cycle assumes that when a perturbation is introduced in two non-interacting residues, X and Y, the effects of each single perturbation are additive in a double mutant where both perturbations are present [37]. Consequently, the change in free energy upon mutating residue X, which is associated with any structural or functional behavior of a given protein, can be expressed as $\Delta\Delta G_{P\text{-}XY\rightarrow P\text{-}Y}$. Analogously, the change in free energy associated with the residue Y will be equal to $\Delta\Delta G_{P\text{-}XY\rightarrow P\text{-}X}$. If the mutations are independent of each other, the double mutant containing both X and Y will exhibit an additive effect of the individual perturbations and:

$$\Delta\Delta G_{P-XY\rightarrow P} = \Delta\Delta G_{P-XY\rightarrow P-Y} + \Delta\Delta G_{P-XY\rightarrow P-X}$$

On the other hand, a non-zero value of $\Delta\Delta\Delta G_{XY}$ would arise from.

$$\Delta\Delta\Delta G_{XY} = \Delta\Delta G_{P-XY\rightarrow P} - \Delta\Delta G_{P-XY\rightarrow P-Y} - \Delta\Delta G_{P-XY\rightarrow P-X}$$

And would correspond to the coupling free energy of interaction between X and Y. In the case of binding experiments performed by stopped-flow analysis, it was shown previously that a reliable value of $\Delta\Delta\Delta G_{XY}$ should exceed the quantity of 0.4 kcal mol^{-1} [26, 35, 37].

In the case of Grb2 allostery, therefore, a double-mutant cycle may be performed by measuring the effects of the presence of the Shp-2 or Irs-1 ligand (perturbation 1), while performing extensive site-directed mutagenesis

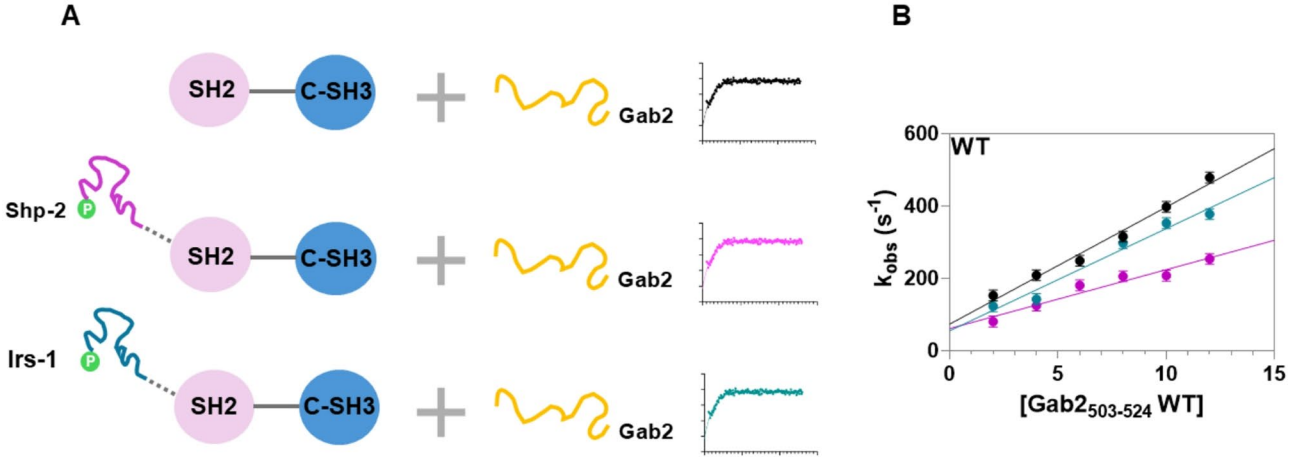

Fig. 1 Kinetic binding experiments between Grb2 and a peptide mimicking $Gab2_{503-524}$. **(A)** A schematic representation of the stopped-flow experiments performed in this work: SH2-SH3 of Grb2 versus a physiological ligand of C-SH3, $Gab2_{503-524}$.The SH2 domain was pre-bound to two distinct ligands, two peptides mimicking the physiological partners of SH2, Shp-2, and Irs-1. **(B)** Kinetic binding experiment performed on Grb2 SH2-SH3 with $Gab2_{503-524}$ in the absence or in the presence of Shp-2 (fuchsia) and Irs-1 (dark-green)

on the C-SH3 domain (perturbation 2). Hence, we engineered 19 site-specific variants of C-SH3, which were then expressed, purified, and analysed through stopped-flow binding experiments, in the absence and in the presence of Shp-2 and Irs-1. The design of these mutants adhered to well-established principles of double-mutant cycles, as detailed previously [26]. In particular, the mutational approach involved the selective deletion of hydrophobic side chains, a mutation type that offers clear interpretability.

The pseudo-first order binding plots of the different variants of SH2-SH3 in isolation and in the presence of an excess of the Irs-1 and Shp-2 peptides are reported in Figs. 2 and 3 respectively and the calculated parameters are reported in Table 1. Importantly, the values obtained are highly consistent with was previously obtained with alternative experimental techniques [38]. To address the allosteric communication between the SH2 and SH3 domains quantitatively, we determined coupling free energies ΔΔΔG by employing thermodynamic and kinetic parameters obtained from binding experiments reported in Figs. 2 and 3, by applying the following equations:

$$\Delta\Delta\Delta\mathrm{G} = \Delta\Delta\mathrm{G}\,\mathrm{eq}SH2 - SH3\,WT^{Gab2(Shp-2)} - \Delta\Delta\mathrm{G}\,\mathrm{eq}\,SH2 - SH3\,mut^{Gab2(Shp-2)}$$

$$\Delta\Delta\Delta\mathrm{G} = \Delta\Delta\mathrm{G}\,\mathrm{eq}\,SH2 - SH3\,WT^{Gab2(Irs-1)} \Delta\Delta\mathrm{G}\,\mathrm{eq}\,SH2 - SH3\,mut^{Gab2(Irs-1)}$$

The ΔΔΔG of all mutants are shown in Table 2. Interestingly, we found that seven residues (Y160A, A163G, H184A, S189A, V210A, T211S, V213A) showed a detectable ΔΔΔG upon mutation, with values of ΔΔΔG > 0.4 kcal mol^{-1}, in the presence of Shp-2. On the other hand, in the presence of Irs-1, no value exceeded 0.4 kcal mol^{-1}. These finding indicate the specific ligands of the SH2 domain exert a different effect on the SH3 and that different ligands modulate the functional coupling

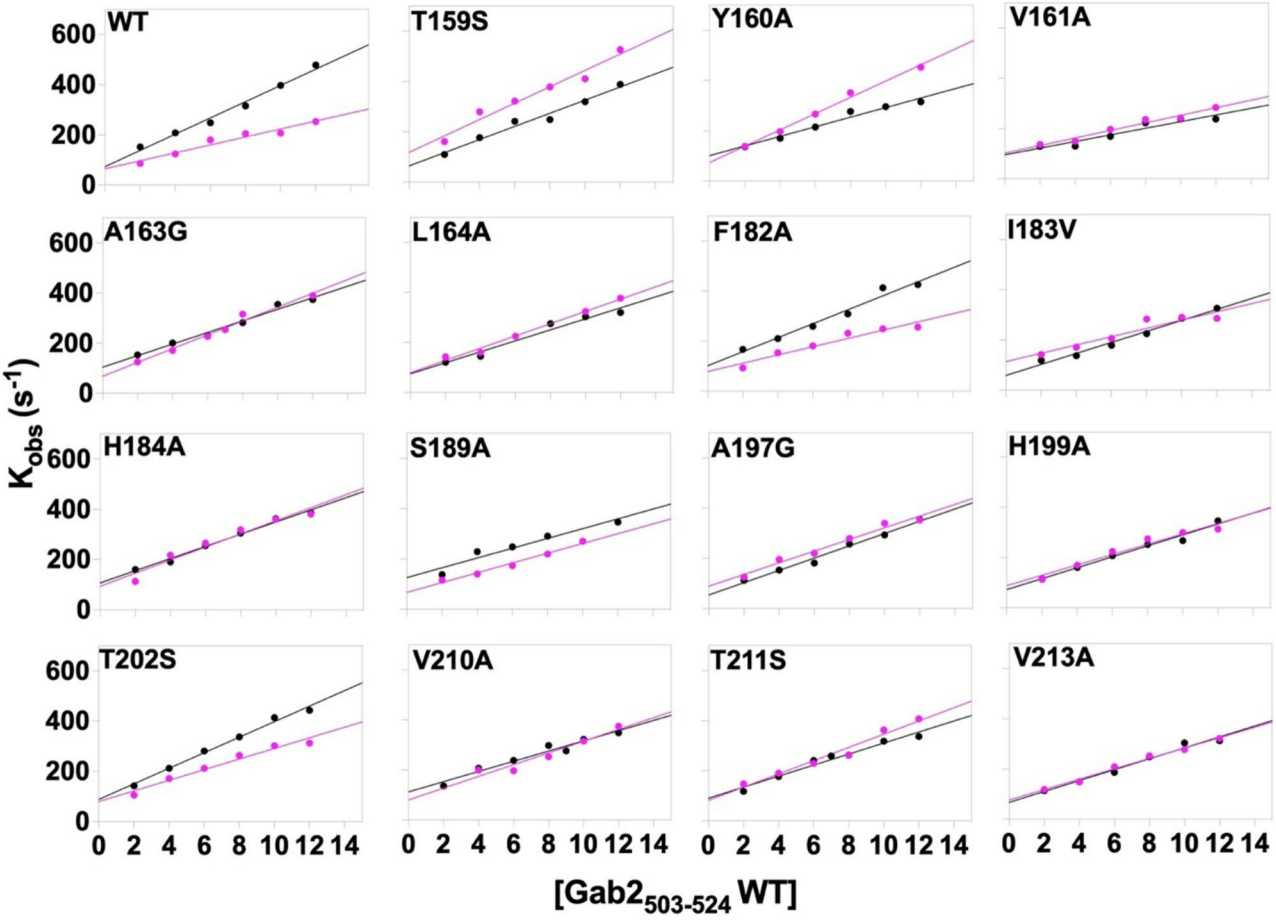

Fig. 2 Kinetic binding experiment between Grb2 SH2–SH3 WT and its site-directed mutants versus $Gab2_{503-524}$ in the absence or in the presence of Shp-2. Kinetic binding experiments were carried out using a stopped-flow apparatus by mixing a constant concentration of Grb2 SH2–SH3 WT or its site-directed mutants with increasing concentrations of $Gab2_{503-524}$ (black-filled circles), as reported in [28], in the absence (black) or in the presence (fuchsia) of saturating concentrations of the peptide mimicking Shp-2

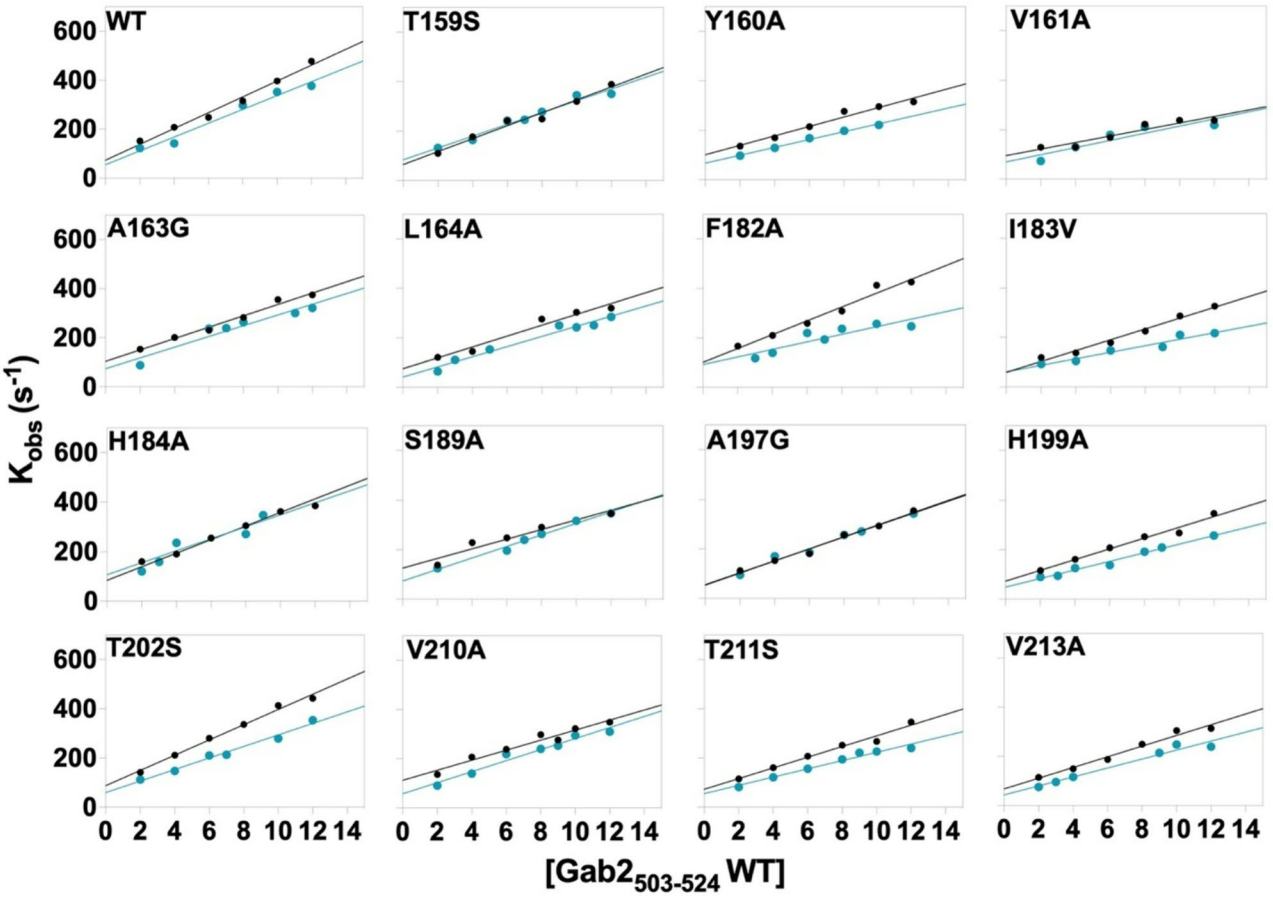

Fig. 3 Kinetic binding experiment with Grb2 SH2–SH3 WT and its site-directed mutants versus $Gab2_{503-524}$ in the absence or in the presence of Irs-1. Kinetic binding experiments were carried out using a stopped-flow apparatus by mixing a constant concentration of Grb2 SH2–SH3 WT or its site-directed mutants with increasing concentrations of $Gab2_{503-524}$ (black-filled circles), as reported in [28], in the absence (black) or in the presence (fuchsia) of saturating concentrations of the peptide mimicking Irs-1 (dark-green)

between SH2 and SH3 in a specific manner, reinforcing the hypothesis of the presence of a fine regulatory mechanism within Grb2, which depend on the type of ligand bound to SH2.

To map differences between the allosteric networks upon ligand binding of SH2, the ΔΔΔG obtained with Shp-2 were subtracted with ΔΔΔG with Irs-1 to obtain a ΔΔΔΔG. This approach, previously introduced to study the communication between the PDZ and GK domains of PSD-95 [39, 40], allows visualizing the structural localization of the allosteric network, which is reported in Fig. 4. Notably, the identified network comprises residues that establish a connection between the binding site of the SH3 domain and the SH2 domain, thereby facilitating allosteric communication between these regions. Importantly, it should be noticed that, as recalled above, allostery may occur even in the absence of conformational changes and should be therefore primarily ascribed to the energetic connections between probed residues.

It is of particular interest to analyze the sign of the calculated ΔΔΔG obtained for Shp-2. With the exception of the variant I183V, displaying in any case a low value of ΔΔΔG, we observed a consistently positive ΔΔΔG value, indicating that the allosteric effects mediated by Shp-2 are more pronounced in the wild-type protein compared to any of the probed mutations. This suggests that the wild-type sequence is inherently optimized to facilitate the propagation of allosteric signals between the SH2 and SH3 domains. The diminished allosteric effects observed in the mutants imply a disruption in the communication network, further reinforcing the notion that the wild-type sequence has evolved to maximize allosteric coupling. This observation is in line with previous findings on PDZ [41] and SH2 [42] domains, underscoring the functional significance of sequence conservation in allosteric regulation. To further monitor whether ligand binding to SH2 correspond to any conformational changes in SH3, we computed an AlphaFold model of the SH2-SH3 tandem and superposed it with the crystal structure of isolated SH3 (Figure S1). Interestingly, the structure of the SH3 domain in the tandem is essentially identical to the crystal structure of SH3. This finding confirms that the

Table 1 Kinetic parameters of the binding reaction of tandem SH2-SH3 wild-type and its site-directed mutants with Gab2 $_{503–524}$ in the absence or in the presence of constant concentration of Irs-1 and Shp-2

SH2-SH3	Gab2 $_{503–524}$			Gab2 $_{503–524}$ (Shp-2)			Gab2 $_{503–524}$ (Irs-1)		
	k_{on} ($\mu M^{-1} s^{-1}$)	k_{off} (s^{-1})	K_D (μM)	k_{on} ($\mu M^{-1} s^{-1}$)	k_{off} (s^{-1})	K_D (μM)	k_{on} ($\mu M^{-1} s^{-1}$)	k_{off} (s^{-1})	K_D (μM)
WT	32 ± 2	70 ± 16	2.3 ± 0.5	16 ± 2	70 ± 10	4.3 ± 0.8	28 ± 3	55 ± 8	1.9 ± 0.3
T159S	26 ± 2	65 ± 17	2.5 ± 0.7	33 ± 3	119 ± 18	3.6 ± 0.7	24 ± 2	84 ± 13	3.5 ± 0.6
Y160A	19 ± 2	102 ± 13	5.3 ± 0.8	32 ± 2	74 ± 11	2.3 ± 0.4	15.9 ± 0.7	68 ± 10	4.3 ± 0.7
V161A	13 ± 2	95 ± 17	7 ± 2	15 ± 1	102 ± 15	7 ± 1	14 ± 4	70 ± 10	5 ± 1
A163G	23 ± 2	104 ± 12	4.5 ± 0.6	28 ± 2	68 ± 10	2.5 ± 0.4	22 ± 3	74 ± 11	3.4 ± 0.7
L164A	22 ± 3	75 ± 21	3 ± 1	24 ± 2	79 ± 12	3.2 ± 0.5	21 ± 2	41 ± 6	2 ± 0.3
F165A*	-	-	-	-	-	-	-	-	-
F167A*	-	-	-	-	-	-	-	-	-
F177A*	-	-	-	-	-	-	-	-	-
F182A	28 ± 2	102 ± 19	3.7 ± 0.7	16 ± 2	79 ± 12	5 ± 1	15 ± 3	93 ± 14	6 ± 2
I183V	22 ± 2	59 ± 12	2.7 ± 0.6	16 ± 3	114 ± 17	7 ± 2	13 ± 2	61 ± 9	4.7 ± 0.9
H184A	24 ± 1	107 ± 11	4.4 ± 0.5	26 ± 3	94 ± 14	3.6 ± 0.7	27 ± 5	84 ± 13	3 ± 0.8
S189A	19 ± 3	126 ± 22	6 ± 2	19 ± 2	67 ± 10	3.5 ± 0.6	23 ± 1	74 ± 11	3.2 ± 0.5
A197G	24 ± 1	54 ± 11	2.2 ± 0.5	23 ± 2	89 ± 13	3.8 ± 0.6	24 ± 2	56 ± 8	2.3 ± 0.4
H199A	22 ± 2	73 ± 13	3.4 ± 0.6	21 ± 2	89 ± 13	4 ± 0.8	17 ± 1	49 ± 7	2.8 ± 0.5
T202S	31 ± 2	88 ± 12	2.8 ± 0.4	21 ± 2	80 ± 12	3.8 ± 0.7	23 ± 2	60 ± 9	2.6 ± 0.4
Y209A*	-	-	-	-	-	-	-	-	-
V210A	20 ± 2	112 ± 16	3.4 ± 0.9	23 ± 4	81 ± 12	3.4 ± 0.8	22 ± 2	58 ± 9	2.6 ± 0.4
T211S	22 ± 2	91 ± 14	4.1 ± 0.7	26 ± 2	82 ± 12	3.1 ± 0.5	17 ± 1	56 ± 8	3.3 ± 0.6
V213A	22 ± 2	67 ± 13	3.1 ± 0.7	21 ± 1	77 ± 12	3.7 ± 0.6	18 ± 2	43 ± 6	2.4 ± 0.4

* In the case of these mutations, we could not obtain any reliable binding trace

Table 2 Coupling free energies between Grb2 SH2-SH3 and Shp-2 and Irs-1

Mutants	ΔΔΔG Shp-2	ΔΔΔG Irs-1	ΔΔΔΔG
T159S	0.14 ± 0.2	-0.28 ± 0.2	0.42 ± 0.3
Y160A	0.82 ± 0.2	0.04 ± 0.2	0.79 ± 0.3
V161A	0.39 ± 0.2	0.14 ± 0.2	0.25 ± 0.3
A163G	0.69 ± 0.2	0.07 ± 0.2	0.62 ± 0.3
L164A	0.38 ± 0.2	0.21 ± 0.2	0.17 ± 0.3
F182A	0.20 ± 0.2	-0.37 ± 0.2	0.58 ± 0.3
I183V	0.18 ± 0.2	-0.39 ± 0.2	0.22 ± 0.3
H184A	0.47 ± 0.2	0.11 ± 0.2	0.35 ± 0.3
S189A	0.70 ± 0.2	0.31 ± 0.2	0.39 ± 0.3
A197G	0.05 ± 0.2	-0.12 ± 0.2	0.16 ± 0.3
H199A	0.21 ± 0.2	0.01 ± 0.2	0.20 ± 0.3
T202S	0.20 ± 0.2	-0.03 ± 0.2	0.22 ± 0.3
V210A	0.62 ± 0.2	0.34 ± 0.2	0.28 ± 0.3
T211S	0.51 ± 0.2	0.03 ± 0.2	0.48 ± 0.3
V213A	0.50 ± 0.2	0.31 ± 0.2	0.18 ± 0.3

Parameters were calculated as described in the text

allosteric behavior detected in our work involves minimal conformational changes.

Probing the different allosteric effects of Shp-2 and Irs-1 phospho-peptides on HEK293 cell line

The results highlighted above suggest a fascinating scenario whereby the allosteric pathways within Grb2 are mediated in a different manner by specific ligands of its central SH2. In this context, it is crucial to note that previous experiments on Grb2 have demonstrated its pivotal role on the activation of the PI3K-Akt pathway [9, 10, 17, 43, 44]. Notably, such activation has been suggested to be synergically activated both by the recognition of phosphopeptides, at the level of the SH2 domain of Grb2 [45–47], and by proline rich segments, such as those displayed by Gab2 and involved in the recognition of the C-SH3 domain (Fig. 5) [2, 48, 49]. Hence, in an effort to provide a validation of our kinetic experiments and to assess their physiological relevance, we performed experiments by exposing HEK293 cell line to the two respective phospho-peptides, mimicking Shp-2 and Irs-1, while monitoring their effects on the PI3K-Akt signaling pathways. These experiments aimed to determine whether the allosteric regulation observed by stopped-flow analysis translates into distinct downstream signaling outcomes within a cellular context. To this end, HEK293 cells were treated with either the Shp-2-mimicking or Irs-1-mimicking peptide, and the activation states of Akt protein was evaluated through quantitative Western blot analysis, using phosphorylation-specific antibodies as readouts for protein activation. To test efficient peptide uptake, performed fluorescence experiments on cell lysates previously threated with dansyl-labelled Irs-1 and Shp-2 peptides. In both cases, we could observe that the fluorescence of the dansyl group could be clearly detected in the cell lysates, with a clear-cut increase in fluorescence as compared to the control. The experimental details are described in the Materials and Methods section.

Given that our biophysical data suggests a ligand-specific modulation of the SH2-SH3 interaction, we hypothesized that these differences might manifest in divergent pathway activation profiles. Our results revealed that stimulation with the Irs-1 mimicking peptide induced a dose-dependent increase in Akt (Ser473) phosphorylation at concentrations of 1 (+ 87%, Fig. 5, B), 5 (+ 152%, Fig. 5, B), and 10 (73%, Fig. 5, B) μM, strongly activating the Akt protein (Fig. 5, A and B). Considering the dose response results, we selected the intermediate dose of 5 μM, that confirmed a significant activation of Ser473-Akt protein induced by Irs-1 peptide (142%, Fig. 5D and E). The Shp-2 [5 μM] peptide showed no significant difference in terms of Akt activation compared to control (Fig. 5, D and E). While the phosphorylation levels of Akt with Shp-2 remained significantly lower compared to those induced by Irs-1 (162%, Fig. 5D and E), suggesting that Shp-2 binding to the SH2 domain of Grb2 likely exerts a more modulatory role, possibly favoring other signaling pathways, rather than directly promoting Akt activation. Remarkably, these experiments corroborate the kinetic analysis, reinforcing the concept that ligand-specific binding to the SH2 domain of Grb2 differentially modulates downstream signaling. Indeed, the stronger Akt activation induced by the Irs-1 peptide aligns with its enhancement of SH3-Gab2 interaction observed in kinetic assays, whereas the modulatory role of the Shp-2 peptide is consistent with its dampening effect on SH3 binding affinity. A schematic representation summarizing this ligand-specific allosteric modulation and its impact on downstream signaling is reported in Fig. 6, providing a visual synthesis of the proposed model.

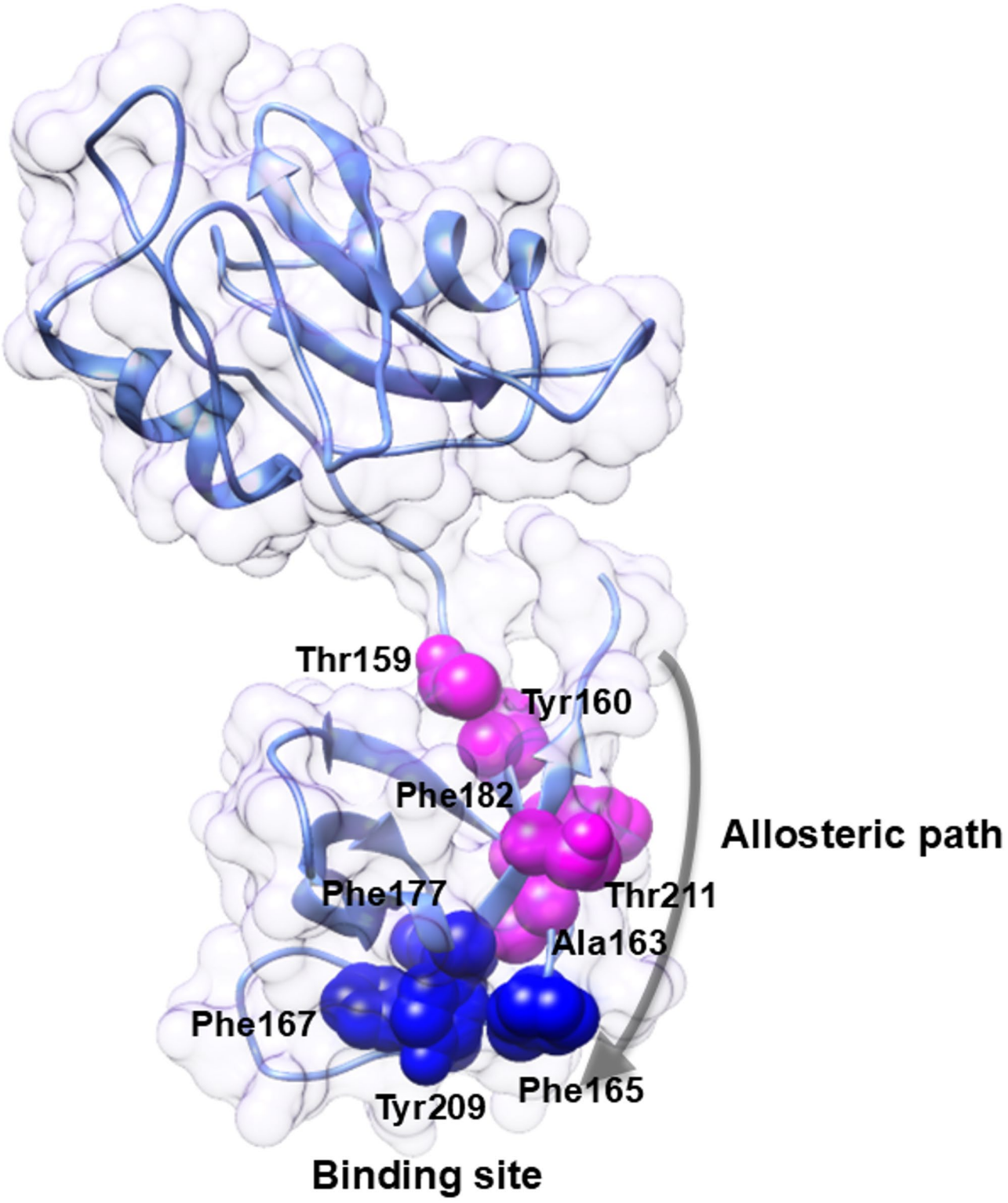

Fig. 4 Allosteric communication within SH2-SH3 Grb2. The image has been obtained by using UCSF Chimera software. (PDB:1GRI). The coupling free energies (ΔΔG) obtained with Irs-1 were subtracted from those of Shp-2 to calculate (ΔΔΔG) allowing visualization of the effect on the allosteric network in SH2-SH3 upon binding of SH2. Mutated residues are represented as spheres. Fuchsia spheres showed a detectable ΔΔΔG with a value > 0.4 kcal mol^{-1}. Blue spheres highlight mutations that abrogate binding with $Gab2_{503–524}$ [28]

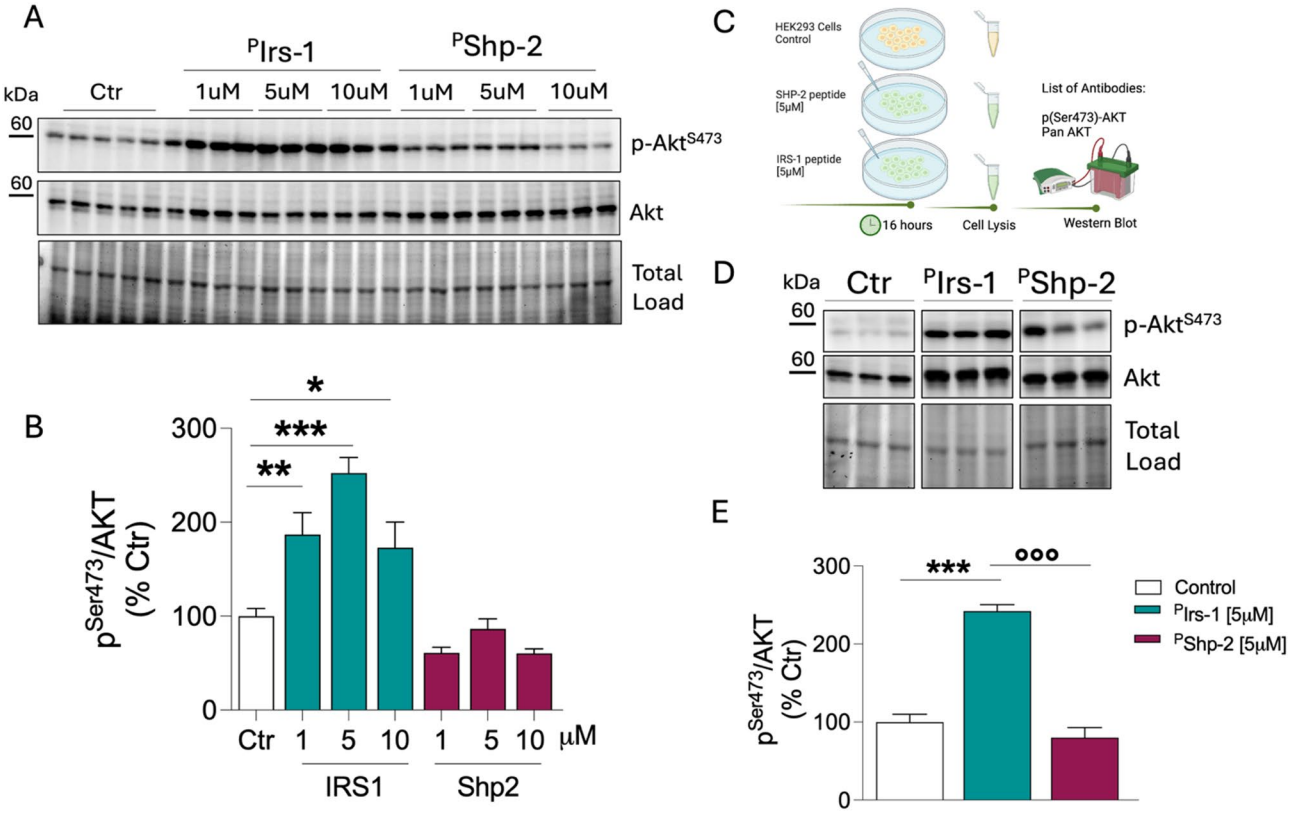

Fig. 5 Effect of Irs-1 and Shp-2 peptide treatment on Akt activation. (**A**) Representative Western blot images and densitometric analysis of (**B**) Akt protein levels and activation (evaluated as the p-Akt^S473/Akt ratio) in HEK cells treated with Irs-1 and Shp-2 peptides at different doses [1, 5, and 10 µM], respectively. (**C**) Depicted treatment on HEK293 cells with Shp-2 and Irs-1 peptides, followed by AKT activation analysis via Western Blot. (**D**) and (**E**) Representative Western blot images and densitometric analysis of (**D**) Akt protein levels and activation (evaluated as the p-Akt^S473/Akt ratio) in HEK cells treated with Irs-1 and Shp-2 peptides at dose of 5 µM. All densitometric values are expressed as a percentage of the control (Ctr), set as 100%, and were normalized to total protein load. Data are presented as mean ± SEM from at least three independent experiments. Statistical analysis was performed using one-way ANOVA followed by Bonferroni's post hoc test: $*p < 0.05$ Ctr vs. Irs-1, $°p < 0.05$ Irs-1 vs. Shp-2

Conclusions

The results reported in this work reinforce the hypothesis that Grb2 is not merely a passive adaptor, but an active integrator of signaling inputs through ligand-specific allosteric modulation. In particular, our kinetic and mutational work allow providing a structural depiction on how the SH2 domain can transmit distinct allosteric cues to the SH3 domain depending on the identity of its bound ligand. This modulation was further validated in a cellular context, where Irs-1 and Shp-2 peptides elicited differential effects on Akt activation, despite their structural similarity. These findings underscore the functional importance of intramolecular communication within modular adaptor proteins and highlight the specificity with which seemingly subtle molecular interactions can influence cell signaling outcomes. Future work on similar adaptor proteins will shed light on the general nature of these effects.

Materials and methods

Protein expression and purification

SH2-SH3(residues 53–217) of the Grb2 protein (Uniprot P62993) was inserted into a pET28b + plasmid vector. Constructs containing site-directed variants of SH2-SH3 were generated by utilizing the gene encoding Grb2-SH2-SH3 wild type as a template. Site-directed mutagenesis was performed using the QuikChange Lightning Site-Directed Mutagenesis kit from Agilent Technologies, according to the instructions of the manufacturer.

Peptides mimicking the region 503 to 524 (YSRGSEIQPPPVNRNLKPDRKAK) of Gab2 and peptides mimicking the region of Irs-1 885–906 (LHPPEPKSPGEpYVNIEFGSDQS), and Shp2 529–551 (EEEQKSKRKGHEpYTNIKYSLAD) were purchased from Genscript Biotech Corp (purity > 90%).

SH2-SH3 WT and all the mutants of the Grb2 protein was expressed and purified as previously reported (Di Felice et al.,2024).

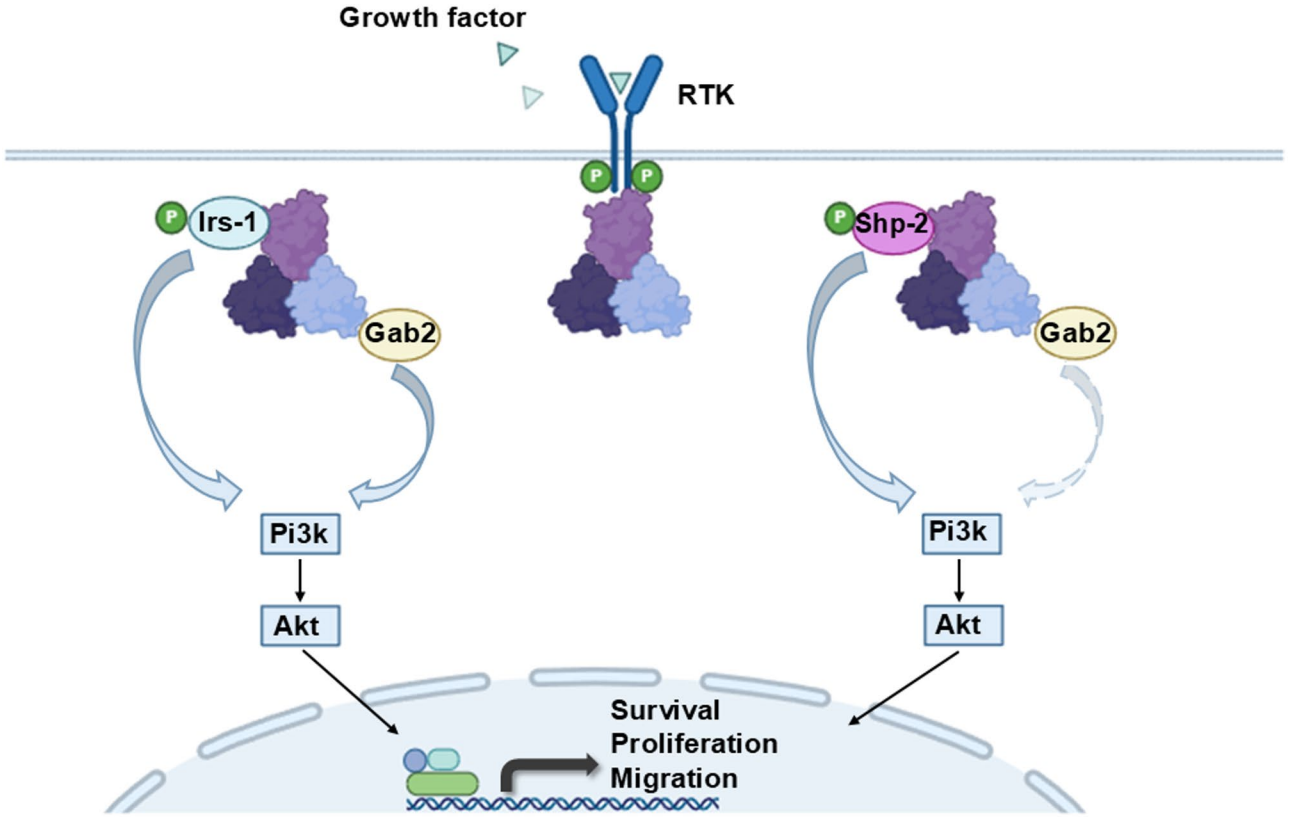

Fig. 6 Ligand-specific allosteric modulation of Grb2. The image offers a simplified sketch summarizing the interactions mediated by Grb2 and leading to the activation of Akt. In particular, both the SH2 domain, via its interaction with phosphorylated ligand such as Shp-2 or Irs-1, and the C-SH3 domain, via its interaction with Gab2, act synergically as promoters for the activation of the Pi3k/Akt pathway. As demonstrated in this work, while the interaction with Irs-1 does not significantly affect the affinity for Gab2, binding to the Shp-2 peptide increases its K_D in a detectable manner

Stopped-flow binding experiments

Kinetic experiments of binding were performed on a single-mixing SX-18 stopped-flow instrument from Applied Photophysics, recording the change of fluorescence emission. The excitation wavelength used was 280 nm while the fluorescence emission was collected using a 320 nm cutoff glass filter. The binding experiments were carried out at 10 °C in pseudo-first order condition mixing a constant concentration of SH2-SH3 Grb2 in the wild-type and mutated forms (2 μM) versus increasing concentrations of $Gab2_{503–524}$ WT (ranging from 2 to 14 μM), in the absence or in the presence of saturating concentrations (10 fold excess of K_D) of $Shp\text{-}2_{529–551}$ and $Irs\text{-}1_{885–906}$. For all measurements the buffer used was 50 mM Hepes, 0.5 M NaCl, pH 7.0. In all cases, an average calculated from 5 to 8 independently acquired kinetic traces was satisfactorily fitted with a single exponential equation to obtain the observed rate constant *k*obs. Dependences of *k*obs as a function of the concentration of Gab2 domain were fitted with the following linear equation:

$$k_{obs} = k_{on}\,[GAB2] + k_{off}$$

Cell culture and treatment

HEK293 cells were cultured in Dulbecco's Modified Eagle's Medium (DMEM) with high glucose (Aurogene, Rome, Italy AU-L0103-500), supplemented with 10% fetal bovine serum (FBS, Sigma Aldrich, St. Louis, MO, USA; F7524) and 1% penicillin-streptomycin solution 100 × (100 IU/ml penicillin and 100 μg/ml streptomycin; Aurogene, Rome, Italy; AU-L0022-100). Cells were maintained at 37 °C in a humidified atmosphere containing 95% air and 5% CO_2. For experiments with Irs-1 $_{885–906}$ and Shp-2 $_{529–551}$ cells were seeded at a density of 8×10^4 cells per well in 24-well plates pre-coated with a poly-L-lysine solution (Sigma-Aldrich, St. Louis, MO, USA, P4707) and treated with different concentrations of each peptide ([1 μM], [5 μM], and [10 μM]) for 24 h in DMEM supplemented with 1% FBS. At the end of the treatment, cells were harvested for biochemical analysis as described below.

To verify peptide uptake, HEK293 cells were plated at the density of 80.000 cells per well. Upon reaching 70–80% confluence, they were treated with a single dose of dansylated peptides (Irs-1 and Shp-2) at a concentration of 5 μM for 24 h, consistent with the dose used in the experimental treatments, described above. All the

analyses were compared to untreated cells (control). At the end of the incubation, cells were washed for 3 times with PBS to eliminate non-internalized peptide and were lysate with RIPA buffer supplemented with protease inhibitors (Sigma-Aldrich, St. Louis, MO, USA, P4707). Lysates were centrifuged for15 min at 12.000 rpm, 4 °C and transferred to flat-bottom plates for fluorescence analysis. Fluorescence was measured using a SpectraMax® reader (Molecular Device) set at 320 nm for excitation and 540 nm for emission. The results revealed a significant increase in danysl fluorescence in cells treated with the Irs-1($17 \pm 3\ 10^5$ Rel.Fl.Un.) and Shp-2 ($5 \pm 1\ 10^5$ Rel.Fl.Un.) peptides compared to control ($1 \pm 03\ 10^5$ Rel. Fl.Un.) indicating substantial intracellular accumulation of the peptides over time.

Samples preparation

Total protein extracts were prepared in radioimmunoprecipitation assay (RIPA) buffer (pH 7.4) containing 50 mM Tris-HCl (pH 7.4), 150 mM NaCl, 1% NP-40, 0.25% sodium deoxycholate, 1 mM EDTA, 0,1% SDS, phosphatase and protease inhibitors (Sigma-Aldrich, St. Louis, MO, USA 1:100, P8340 and P5726, respectively). Then, samples were homogenized by 20 strokes of a Wheaton tissue homogenizer, sonicated, and centrifuged at 14 000 rpm for 30 min at 4 °C to remove debris. Supernatant was collected and total protein concentration was determined by the BCA method according to manufacturer's instructions (Pierce, Rockford, IL, USA, 23227).

Western blot

For Western blot analysis, 15 µg of proteins were separated by 4–15% gradient sodium dodecyl sulfate–polyacrylamide gel electrophoresis (SDS-PAGE), using Criterion TGX (Tris-Glycine extended) Stain-Free precast gels (Bio-Rad, Hercules, CA, USA) in Tris/Glycine/SDS (TGS) Running Buffer (Bio-Rad Laboratories, #1610772). All the samples were loaded on the same gel by using 26-well gel (Bio-Rad Laboratories, 5678085). Immediately after electrophoresis, the gel was then placed on a Chemi/UV/Stain-Free tray and then placed into a ChemiDoc MP imaging System (Bio-Rad Laboratories, 17001402) and UV-activated based on the appropriate settings with Image Lab Software (Bio-Rad Laboratories) to collect total protein load image. Following electrophoresis and gel imaging, the proteins were transferred via the TransBlot Turbo semi-dry blotting apparatus (Bio- Rad Laboratories, #1704150) onto nitrocellulose membranes (Bio-Rad, Hercules, CA, USA, #162–0115). Membranes were blocked with 5% of Blotto Immunoanalytical Grade Non-Fat Dry Milk (SERVA, Heidelberg, Germany, 42590.01) in TBS solution containing 0.01% Tween 20 (T-TBS) and incubated over night at 4 ∘C with primary antibodies (anti-Akt-phospho Ser473, #4058S, Cell Signaling Technologies and anti-Akt N-terminal region, #AM1011, ECM Biosciences) diluted 1:1000 in blocking solution Subsequently, membranes were incubated with horseradish peroxidase-conjugated secondary antibodies diluted 1:10000 in T-TBS solution for 1 h at room temperature (anti-rabbit IgG #L005661, anti-mouse IgG #L005662, Bio-Rad Laboratories, Hercules, CA, USA). Membranes were developed with Clarity enhanced chemiluminescence (ECL) substrate (Bio-Rad Laboratories, Hercules, CA, USA, #1705061) and then acquired with ChemiDoc MP (Bio-Rad, Hercules, CA, USA) and analyzed using Image Lab 6.1 software (Bio-Rad, Hercules, CA, USA) that allows the normalization of a specific protein signal by the total protein load. Total protein staining measures the aggregate protein signal (sum) in each lane and eliminates the error that can be introduced by a single internal control protein. Total protein staining is a reliable and applicable strategy for quantitative immunoblotting. It directly monitors and compares the aggregate amount of sample protein in each lane, rather than using an internal reference protein as a surrogate marker of sample concentration. This direct, straightforward approach to protein quantification may increase the accuracy of normalization. Total load can be detected by taking advantage of stain-free technology (BioRad, Hercules, CA, USA). Stain-free imaging technology utilizes a proprietary trihalo compound to enhance natural protein fluorescence by covalently binding to tryptophan residues with a brief UV activation. Images of the gel or membrane after transfer can easily be captured multiple times without staining and destaining steps.

Statistical analysis

Statistical analyses were performed by using one-way ANOVA analysis with Bonferroni multiple comparison tests for the evaluation of differences between more than two groups. All statistical tests were two-tailed, and the level of significance was set at 0.05. Data are expressed as mean ± SEM per group from at least three independent experiments and details about each test are reported in figure legend. All statistical analyses were performed using Graph Pad Prism 10.0 software (GraphPad, La Jolla, CA, USA).

Supplementary Information

The online version contains supplementary material available at https://doi.org/10.1186/s13062-025-00656-5.

Supplementary Material 1

Author contributions

M.d.F., and S.G. designed research; M.d.F., L.R.R., J.T., V.P., E.S.V, performed research; M.d.F., L.R.R., A.To, A.Tr., S.G., analyzed data; A.To, A.Tr., S.G. supervised

research; M.d.F., A.Tr. and S.G. wrote the first version of the manuscript and all authors read and approved the manuscript.

Funding
This work was partly supported by grants from European Union's MSCA Doctoral Networks under the Grant Agreement IDPro No 101,119,633 (to S.G.), by grants from Sapienza University of Rome (RG12017297FA7223, RG1231888A88129D to S.G., RG124190E53A81B8, RM12218148DA1933 to A.T.), the Associazione Italiana per la Ricerca sul Cancro (Individual Grant—IG 24551 to S.G.), the Istituto Pasteur Italia ("Research Program 2022 to 2023 Under 45 Call 2020" to A.T.), the Italian MUR-PRIN 2022 grant N. 2022JY3PMB to A.T. We acknowledge co-funding from Next Generation EU, in the context of the National Recovery and Resilience Plan, and the Investment PE8—Project Age-It: "Ageing Well in an Ageing Society", and the European Union – Next GenerationEU (Project ECS 0000024 Rome Technopole, – CUP B83C22002820006, NRP Mission 4 Component 2 Investment 1.5 to L.R.R.). This resource was co-financed by the Next Generation EU [DM 1557 11 October 2022]. The views and opinions expressed are only those of the authors and do not necessarily reflect those of the European Union or the European Commission. Neither the European Union nor the European Commission can be held responsible for them.

Data availability
No datasets were generated or analysed during the current study.

Declarations

Competing interests
The authors declare no competing interests.

Received: 14 April 2025 / Accepted: 18 May 2025
Published online: 23 May 2025

References

1. Bai Y, Wang H, Li C. SAPAP scaffold proteins: from synaptic function to neuropsychiatric disorders. Cells. 2022;11:3815.
2. Lewitzky M, Simister PC, Feller SM. Beyond 'furballs' and 'dumpling soups'-towards a molecular architecture of signaling complexes and networks. FEBS Lett. 2012;586:2740–50.
3. Paul S, Biswas SR, Milner JP, Tomsick PL, Pickrell AM. Adaptor-Mediated trafficking of tank binding kinase 1 during diverse cellular processes. Traffic. 2025;26:e70000.
4. Smith MR, Costa G. Insights into the regulation of mRNA translation by scaffolding proteins. Biochem Soc Trans. 2024;52:2569–78.
5. Hirschi S, Ward TR, Meier WP, Müller DJ, Fotiadis D. Synthetic biology: Bottom-Up assembly of molecular systems. Chem Rev. 2022;122:p16294–16328.
6. Luo LY, Hahn WC. Oncogenic signaling adaptor proteins. J Genet Genomics. 2015;42:512–29.
7. Zhu J, Shang Y, Zhang M. Mechanistic basis of MAGUK-organized complexes in synaptic development and signalling. Nat Rev Neurosci. 2016;17:209–23.
8. Buday L, Downward J. Epidermal growth factor regulates p21ras through the formation of a complex of receptor, Grb2 adapter protein, and Sos nucleotide exchange factor. Cell. 1993;73:611–20.
9. Lowenstein EJ, Daly RJ, Batzer AG, Li W, Margolis B, Lammers R, Ullrich A, Skolnik EY, Bar-Sagi D, Schlessinger J. The SH2 and SH3 domain-containing protein GRB2 links receptor tyrosine kinases to Ras signaling. Cell. 1992;70:431–42.
10. Skolnik EY, Batzer A, Li N, Lee CH, Lowenstein E, Mohammadi M, Margolis B. The function of GRB2 in linking the insulin receptor to Ras signaling pathways. Science. 1993;260:1953–5.
11. Tari AM, Lopez-Berestein G. GRB2: a pivotal protein in signal transduction. Semin Oncol. 2001;28:142–7.
12. Malagrinò F, Coluccia A, Bufano M, Regina G, Puxeddu M, Toto A, Visconti L, Paone A, Magnifico MC, Troilo F, Cutruzzolà F, Silvestri R, Gianni S. Targeting the interaction between the SH3 domain of Grb2 and Gab2. Cells. 2020;9:9112435.
13. Ijaz M, Wang F, Shahbaz M, Jiang W, Fathy AH, Nesa EU. The role of Grb2 in Cancer and peptides as Grb2 antagonists. Protein Pept Lett. 2018;24:1084–95.
14. Malagrinò F, Puglisi E, Pagano L, Travaglini-Allocatelli C. GRB2: A dynamic adaptor protein orchestrating cellular signaling in health and disease. Biochem Biophys Rep. 2024;39:101803.
15. Nishida K, Hirano T. The role of Gab family scaffolding adapter proteins in the signal transduction of cytokine and growth factor receptors. Cancer Sci. 2003;94:1029–33.
16. Wang D, Liu G, Meng Y, Chen H, Ye Z, Jing J. The configuration of GRB2 in protein interaction and signal transduction. Biomolecules. 2024;14:259.
17. Li Z, Zhao PL, Gao X, Li X, Meng YQ, Li ZQ, Zhai KR, Wei SL, Feng HM, Huang HR, Li B. DUS4L suppresses invasion and metastasis in LUAD via modulation of PI3K/AKT and ERK/MAPK signaling through GRB2. Int Immunopharmacol. 2024;143:113043.
18. Maignan S, Guilloteau JP, Fromage N, Arnoux B, Becquart J, Ducruix A. Crystal structure of the mammalian Grb2 adaptor. Science. 1995;268:291–3.
19. Kaynak BT, Dahmani ZL, Doruker P, Banerjee A, Yang SH, Gordon R, Itzhaki LS, Bahar I. Cooperative mechanics of PR65 scaffold underlies the allosteric regulation of the phosphatase PP2A. Structure. 2023;31:607–18.
20. Nussinov R, Jang H. The value of protein allostery in rational anticancer drug design: an update. Expert Opin Drug Discov. 2024;19:1071–85.
21. Perez-Riba A, Synakewicz M, Itzhaki LS. Folding cooperativity and allosteric function in the tandem-repeat protein class. Philos Trans R Soc Lond B Biol Sci. 2018;373:20170188.
22. Monod J, Changeux J-P, Jacob F. Allosteric proteins and cellular control systems. J Mol Biol. 1963;6:306–9.
23. Monod J, Wyman J, Changeux J-P. On the nature of allosteric transitions: A plausible model. J Mol Biol. 1965;12:88–118.
24. Cooper A, Dryden DT. Allostery without conformational change. A plausible model. Eur Biophys J. 1984;11:103–9.
25. Gianni S, Jemth P. Allostery frustrates the experimentalist. J Mol Biol. 2023;435:167934.
26. Pagano L, Toto A, Malagrinò F, Visconti L, Jemth P. Double mutant cycles as a tool to address folding, binding, and allostery. Int J Mol Sci. 2021;22:828.
27. Roy M, Horovitz A. Distinguishing between concerted, sequential and barrierless conformational changes: folding versus allostery. Curr Opin Struct Biol. 2024;83:102721.
28. Di Felice M, Pagano L, Pennacchietti V, Diop A, Pietrangeli P, Marcocci L, Di Matteo S, Malagrinò F, Toto A. The binding selectivity of the C-terminal SH3 domain of Grb2, but not its folding pathway, is dictated by its contiguous SH2 domain. J Biol Chem. 2024;300:107129.
29. Kazemein Jasemi NS, Herrmann C, Magdalena Estirado E, Gremer L, Willbold D, Brunsveld L, Dvorsky R, Ahmadian MR. The intramolecular allostery of GRB2 governing its interaction with SOS1 is modulated by phosphotyrosine ligands. Biochem J. 2021;478:2793–809.
30. McDonald CB, Hokayem JE, Zafar N, Balke JE, Bhat V, Mikles DC, Deegan BJ, Seldeen KL, Farooq A. Allostery mediates ligand binding to Grb2 adaptor in a mutually exclusive manner. J Mol Recogn. 2013;26:92–103.
31. Adams SJ, Aydin IT, Celebi JT. GAB2–a scaffolding protein in cancer. Mol Cancer Res. 2012;10:1265–70.
32. Ding CB, Yu WN, Feng JH, Luo JM. Structure and function of Gab2 and its role in cancer. Mol Med Rep. 2015;12:4007–14.
33. Zhao C, Yu DH, Shen R, Feng GS. Gab2, a new pleckstrin homology domain-containing adapter protein, acts to uncouple signaling from ERK kinase to Elk-1. J Biol Chem. 1999;274:19649–54.
34. Malagrinò F, Troilo F, Bonetti D, Toto A, Gianni S. Mapping the allosteric network within a SH3 domain. Sci Rep. 2019;9:8279.
35. Horovitz A. Double-mutant cycles: a powerful tool for analyzing protein structure and function. Fold Des. 1996;1:R121–6.
36. Serrano L, Horovitz A, Avron B, Bycroft M, Fersht AR. Estimating the contribution of engineered surface electrostatic interactions to protein stability by using double-mutant cycles. Biochemistry. 1990;29:9343–52.
37. Schreiber G, Fersht AR. Energetics of protein-protein interactions: analysis of the barnase-barstar interface by single mutations and double mutant cycles. J Mol Biol. 1995;248:478–86.
38. Faure AJ, Domingo J, Schmiedel JM, Hidalgo-Carcedo C, Diss G, Lehner B. Mapping the energetic and allosteric landscapes of protein binding domains. Nature. 2022;604:175–83.
39. Laursen L, Gianni S, Jemth P. Dissecting Inter-domain cooperativity in the folding of a multi domain protein. J Mol Biol. 2021;433:167148.
40. Laursen L, Kliche J, Gianni S, Jemth P. Supertertiary protein structure affects an allosteric network. Proc Natl Acad Sci U S A. 2020;433:p167148.
41. Gianni S, Haq SR, Montemiglio LC, Jürgens MC, Engström Å, Chi CN, Brunori M, Jemth P. Sequence-specific long range networks in PSD-95/

discs large/ZO-1 (PDZ) domains tune their binding selectivity. J Biol Chem. 2011;286:27167–75.
42. Diop A, Santorelli D, Malagrinò F, Nardella C, Pennacchietti V, Pagano L, Marcocci L, Pietrangeli P, Gianni S, Toto A. SH2 domains: folding, binding and therapeutical approaches. Int J Mol Sci. 2022;23:15944.
43. Gao X, Long R, Qin M, Zhu W, Wei L, Dong P, Chen J, Luo J, Feng J. Gab2 promotes the growth of colorectal cancer by regulating the M2 polarization of tumor–associated macrophages. Int J Mol Med. 2024;53:3.
44. Xu L, Ding R, Song S, Liu J, Li J, Ju X, Ju B. Single-cell RNA sequencing reveals the mechanism of PI3K/AKT/mTOR signaling pathway activation in lung adenocarcinoma by KRAS mutation. J Gene Med. 2024;26:3658.
45. Najib S, Sánchez-Margalet V. Sam68 associates with the SH3 domains of Grb2 recruiting GAP to the Grb2-SOS complex in insulin receptor signaling. J Cell Biochem. 2002;86:99–106.
46. Pruett W, Yuan Y, Rose E, Batzer AG, Harada N, Skolnik E. Association between GRB2/Sos and insulin receptor substrate 1 is not sufficient for activation of extracellular signal-regulated kinases by interleukin-4: implications for Ras activation by insulin. Mol Cell Biol. 1995;15:1778–85.
47. Salameh A, Galvagni F, Bardelli M, Bussolino F, Oliviero S. Direct recruitment of CRK and GRB2 to VEGFR-3 induces proliferation, migration, and survival of endothelial cells through the activation of ERK, AKT, and JNK pathways. Blood. 2005;106:3423–31.
48. He Y, Nakao H, Tan SL, Polyak SJ, Neddermann P, Vijaysri S, Jacobs BL, Katze MG. Subversion of cell signaling pathways by hepatitis C virus nonstructural 5A protein via interaction with Grb2 and P85 phosphatidylinositol 3-kinase. J Virol. 2002;76:9207–17.
49. Weinger JG, Gohari P, Yan Y, Backer JM, Varnum B, Shafit-Zagardo B. In brain, Axl recruits Grb2 and the p85 regulatory subunit of PI3 kinase; in vitro mutagenesis defines the requisite binding sites for downstream Akt activation. J Neurochem. 2008;106:134–46.

Publisher's note